

# $\gamma$ -MnO<sub>2</sub> for Li batteries

## Part I. $\gamma$ -MnO<sub>2</sub>: Relationships between synthesis conditions, material characteristics and performances in lithium batteries

S. Sarciaux<sup>\*</sup>, A. Le Gal La Salle, A. Verbaere, Y. Piffard, D. Guyomard

*Institut des Matériaux de Nantes, UMR CNRS-Université de Nantes no. 6502, 2, rue de la Houssinière-BP 32229, 44322 Nantes Cedex 3, France*

### Abstract

With the use of various electrodeposition conditions (concentration and pH of the bulk MnSO<sub>4</sub> solution, temperature, synthetic mode) and thermal treatments,  $\gamma$ -MnO<sub>2</sub> materials exhibiting rather different physico-chemical and structural characteristics were prepared. Relationships were established between synthesis conditions and such characteristics, showing that to some extent, these physico-chemical and structural parameters can be tuned. The electrochemical behavior of lithiated phases obtained upon the first Li insertion into these  $\gamma$ -MnO<sub>2</sub> materials has been investigated. It is shown that the maximum Li reversible intercalation capacity strongly depends on the structural parameters (concentration of De Wolff defects and degree of microtwinning) of the starting  $\gamma$ -MnO<sub>2</sub> samples. © 1999 Elsevier Science S.A. All rights reserved.

*Keywords:*  $\gamma$ -MnO<sub>2</sub>; Electrodeposition; Characterization; Li insertion; Cycling behavior

### 1. Introduction

Among the large variety of manganese oxides,  $\gamma$ -MnO<sub>2</sub> materials are widely used in primary and secondary alkaline batteries. Their use as positive electrode for rechargeable lithium batteries requires a dehydration between 250 and 400°C and the materials are then called HTMD (Heat Treated Manganese Dioxides).

The structure of  $\gamma$ -MnO<sub>2</sub> is characterized by varying proportions of two types of random structural defects, namely de Wolff defects and microtwinning [1]. De Wolff defects correspond to intergrowths of rutile-type structural units within the ramsdellite structure (Pr is the rutile concentration). Packing faults are generated by (021) and (061) twinning planes within the ramsdellite structure, as well as (011) and (031) twinning planes within the rutile structure (Tw is the overall amount of microtwinning). Consequently, the structural characterization of  $\gamma$ -MnO<sub>2</sub> materials by diffraction techniques is complex and requires simulation of the powder patterns with the Diffax program [2].

EMDs (Electrochemical Manganese Dioxides) are usually prepared by oxidative electrodeposition at high constant current density from acidic MnSO<sub>4</sub> solutions, at temperatures close to 100°C. They typically have a microtwinning degree of more than 80% and about 40 to 50% de Wolff defects [1].

Within a research program devoted to the understanding of the influence of  $\gamma$ -MnO<sub>2</sub> synthetic conditions on the Li insertion behavior, the electrodeposition parameters were varied: MnSO<sub>4</sub> concentration, pH of the bulk solution, temperature, synthetic mode (constant current or voltage, scanning current or voltage) and annealing process. We report here on relationships between such conditions, materials characteristics and performances in lithium batteries.

### 2. Experimental

The oxide materials were deposited from stirred solutions either by potentiostatic or galvanostatic electrolysis for several hours at constant potential (P mode) or current (G mode), or by scanning potentials (SP mode) or currents (SG mode) between two chosen values (noted  $E_{\text{ox}}$  and  $E_{\text{red}}$  in SP mode, or  $J_{\text{ox}}$  and  $J_{\text{red}}$  in SG mode). Various

<sup>\*</sup> Corresponding author

$(E_{\text{ox}}, E_{\text{red}})$  or  $(J_{\text{ox}}, J_{\text{red}})$  couples were selected to get various  $RQ = Q_{\text{ox}}/Q_{\text{red}}$  ratios, where  $Q_{\text{ox}}$  and  $Q_{\text{red}}$  represent the total oxidation and reduction quantities of electricity, respectively. Various electrodeposition temperatures were used. Experimental conditions were always chosen so that the material electrodeposition onto the electrode surface did not affect the solution concentration by more than 5% [3].

After being collected by scraping the Pt electrode, samples were first rinsed with distilled water and then dried at room temperature in a desiccator under  $P_2O_5$  during the time needed for their mass to become constant (between 24 and 48 h). An annealing procedure at various temperatures was used in order to dehydrate the samples in view of further Li insertion experiments. A combination of TGA and redox titrations [4] was used to determine the general formulation  $MnO_y \cdot nH_2O$  of the  $\gamma$ - $MnO_2$  materials thus characterizing their physico-chemical parameters  $y$  and  $n$ .

X-Ray Diffraction (XRD) patterns were recorded on a Siemens D5000 diffractometer using  $Cu\ K\alpha$  radiation. Structural characterization of materials was performed from these patterns, first according to a method recently proposed by Chabre and Pannetier in order to determine Pr and Tw values of  $\gamma$ - $MnO_2$  [1]. The formulas given by Pannetier to estimate Tw were established for Pr = 0%, and corrections were proposed for higher Pr values. However, the applicability becomes difficult when Pr is high. Consequently, Pr and Tw values were determined with the use of an extension of Pannetier's method, based on the simulation of XRD patterns of  $\gamma$ - $MnO_2$  in which the two types of defects are present simultaneously, and recently elaborated in our group [5,6]. Furthermore, as only one possible distribution of microtwinning was considered in previous simulations [1] (although their number is theoretically unlimited), other possibilities were examined and a comprehensive analysis of this problem is given in Ref. [5] and will be further described elsewhere [6]. As a matter of fact, a single (021) twinning plane in a ramsdellite crystal generates two symmetrical twin components P1 and P2 related by the (021) mirror plane. Each time that a twinning occurs in a P1-type component, it induces a local P1  $\rightarrow$  P2 change (and conversely a local P2  $\rightarrow$  P1 change if it occurs in a P2-type component). Let  $\alpha$  be the probability of a P1  $\rightarrow$  P2 change and  $\beta$  that of a P2  $\rightarrow$  P1 change; it appears that possible distributions of microtwinning are defined by the  $\alpha$  and  $\beta$  values. In previous simulations [1], a model with  $\alpha = 1 - \beta$  was taken, leading to a microtwinning degree  $Tw = 200\alpha\%$ . Another model corresponding to  $\alpha = \beta$  was thoroughly investigated [5,6]. It leads to a microtwinning degree hereafter noted Mt, with  $Mt = 100\alpha\%$ . A crude correspondence between Mt and Tw is then given by  $Mt' = Tw/2$ . However, these two models are different even though they lead to rather similar simulations. It appears for example, that  $Tw = 100\%$  does not correspond to the maximum possible

degree of microtwinning. Consequently, in the following the new model is preferred and the structural parameter Mt is used instead of Tw.

Composite electrodes were prepared by mixing the active material, a carbon black (Super-P from Chemetals, Baltimore, MD, USA) and a binder (polyvinylidene difluoride: PVDF) with the massic ratio (85:10:5) and coating the mixture onto an Al disk serving as the current collector.

Standard laboratory swagelok test cells were used with the composite electrode as the positive and Li metal as the negative, separated with glass paper soaked in the electrolyte. The electrolyte was made of 1 M  $LiPF_6$  dissolved in a 2:1 mixture of ethylene carbonate (EC) and dimethyl carbonate (DMC). The cells were tested using the Mac-Pile system operating in galvanostatic or potentiodynamic mode.

### 3. Results and discussion

#### 3.1. Relationships between material characteristics and synthesis conditions

Fig. 1 shows the evolution of the oxygen content  $y$  vs. current density at two temperatures. Other experimental parameters, such as concentration of  $MnSO_4$ , pH, or synthesis mode (P, G, SG or SP) do not influence the  $y$  value. One can observe that  $y$  decreases as the current density increases, with a faster evolution as the synthesis temperature decreases. At room temperature, very low current densities are required in order to prepare fully oxidized EMD, whereas at  $97^\circ C$ , this kind of compound is obtained whatever the current density [3]. Our results are in agreement with general trends observed for electrodeposited  $\gamma$ - $MnO_2$  prepared between  $87$  and  $100^\circ C$  [7,8]. However, to our knowledge, no investigation is mentioned in the literature concerning the variation of  $y$  with the experimental parameters, for an electrodeposition at room temperature.

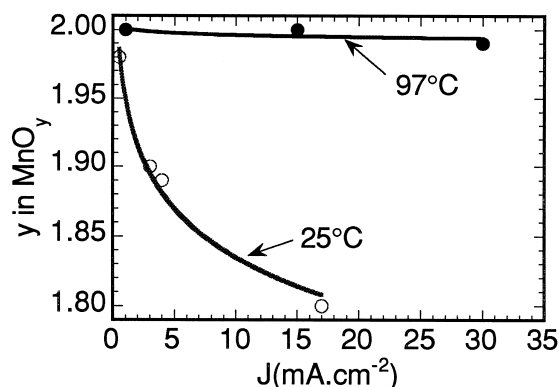


Fig. 1. Variations of  $y$  in the general formula  $MnO_y \cdot nH_2O$  with the current density used for electrodeposition.

The TG and DSC experiments performed with electrodeposited  $\gamma$ -MnO<sub>2</sub> show that the dehydration process occurs in three distinct steps as mentioned in the succeeding paragraphs below.

(1) An important release of loosely bonded water occurs between 25 and 200°C, corresponding to an endothermic process.

(2) Between 200 and  $\sim$ 500°C, a second weight loss and two endothermic processes are observed. They are associated to the release of more strongly bonded water (coordination water) and the simultaneous complete oxidation of Mn to the +IV state (for the samples with  $y < 2$  prepared below 97°C). It appears that the amount of coordination water decreases when  $y$  increases [3] in agreement with the interpretation of Ruetschi [9].

(3) At 450–560°C (depending on the sample) a new weight loss, corresponding to an endothermic process, is observed. It leads to the formation of Mn<sub>2</sub>O<sub>3</sub> that was identified from its XRD pattern.

XRD patterns of electrodeposited  $\gamma$ -MnO<sub>2</sub> (an example is given in Fig. 2) were analyzed in order to determine the Pr and Mt structural parameters. This analysis allows to highlight correlations. For the P and G synthesis modes, the following correlations apply.

—Whatever the synthesis temperature, the increasing of the bulk solution pH from 1.8 to 3.5 seems to lead to smaller values of Pr. It must be mentioned that experiments at pH > 4 were avoided because of Mn(OH)<sub>2</sub> precipitation.

—Samples are noted to contain between 35 and 50% of intergrowth of rutile-type structural units and are strongly microtwinned (Mt  $\geq$  80%), except if synthesis is performed at low electrodeposition current density. This result is in accordance with the work of Poinson et al. [10], showing that samples with Mt  $\approx$  10% can be obtained at 97°C by using a current density less than 0.05 mA cm<sup>-2</sup>. Such samples were not prepared in this work, because of the excessive preparation time necessary to obtain a quantitative amount of product.

—A decrease of the current density of electrodeposition, allows to get lower values of Mt and leads to better crystallized samples.

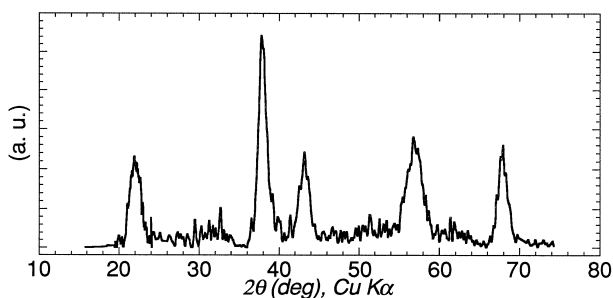


Fig. 2. XRD pattern of a sample with Pr = 35% and Mt = 80%.

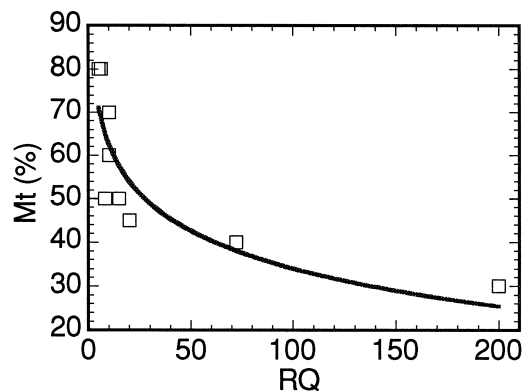


Fig. 3. Variations of the Mt values of different samples from SP and SG mode with the ratio  $RQ = Q_{ox} / Q_{red}$  of the respective oxidation and reduction quantities of electricity.

In the case of SP and SG synthesis modes, it clearly appears that the Pr and Mt values do not depend on the same experimental parameters.

—It is not the average current density which has an influence upon the Mt values but the RQ ratio, as shown in Fig. 3. The highlighted influence of the bulk solution pH upon Pr in the P and G modes, is not observed with scanning current or voltage experiments, because of local pH variations [3].

—The samples synthesized in SP or SG mode present values of Mt which are lower than for samples prepared in P or G mode at equivalent average current. Then, the SG or SP experiments allow to obtain EMDs with low Mt values more quickly.

Prior to their use in lithium batteries  $\gamma$ -MnO<sub>2</sub> are usually dehydrated at temperatures between 250°C and 400°C [11–13]. This treatment induces structural modifications characterized by an increase of Pr and a decrease of Mt. Simultaneously, a complete oxidation of Mn to the +IV state is observed.

Various annealing processes were applied to EMDs prepared in the course of this study and to a CMD (Chemical Manganese Dioxide) with a dominant ramsdellite character (obtained from Sedema), leading to the following results below.

—A thermal treatment at  $T \geq 350^\circ\text{C}$  in air for 8 h leads to structural parameters that are similar to those of classical HTMDs.

—Upon heating in air for 6 days at lower temperature (250°C), samples with initial Pr < 50% lead to unusually small Pr values and/or unusually large Mt values with respect to values already reported for HTMDs [1]. In other words, upon a mild thermal treatment, the structural evolution towards the  $\beta$ -MnO<sub>2</sub> structure can be minimized.

From the investigations mentioned above, many different  $\gamma$ -MnO<sub>2</sub> samples (in terms of structural parameters Pr and Mt) have been prepared.

### 3.2. Relationships between performances in Li batteries and material characteristics

Electrochemical investigations on various  $\gamma$ -MnO<sub>2</sub> compounds (in terms of physico-chemical and structural parameters) were undertaken in order to find out correlations between the maximum Li reversible intercalation capacity of and material characteristics.

The curve shown in Fig. 4 corresponds to a typical electrochemical behaviour during the first lithium insertion–deinsertion cycle, for HTMD samples with  $y = 2$ . The first lithium insertion occurs at about 2.8 V. The shape of the  $U-x$  curve changes completely between the first and the second discharge. This difference is the consequence of a first-order reaction, otherwise said a two-phased mechanism, leading to a new lithiated phase during the first insertion of lithium.

In order to evaluate the influence of Pr and Mt on the cycling behavior, various samples sieved between 1 and 5  $\mu\text{m}$  were subjected to insertion–deinsertion cycles in galvanostatic mode with a C/6 rate and the Li intercalation capacities were compared. Two types of evolutions were identified (experiments done in galvanostatic mode at a C/6 rate) which can be illustrated (Fig. 5), by the behavior of HTMD sample (1) (Pr = 45%, Mt = 8%,  $y = 2$ ) and sample (2) (Pr = 95%, Mt = 3%,  $y = 2$ ) which are almost anhydrous.

–For sample (1) with the smallest Pr value (Pr = 45%) the capacity decreases rather rapidly over the first 10 cycles, and then more slowly.

–For HTMD samples with large Pr contents, like sample (2), the important decrease of the capacity at the second discharge is followed by an increase upon cycling before stabilizing at a maximum value after about 10 cycles (th. This is interpreted as a more difficult transformation of the starting compound into the final lithiated phase (see Part II).

The influence of the water content on the cycling behavior is illustrated (Fig. 5) by sample (3) (Pr = 35%,

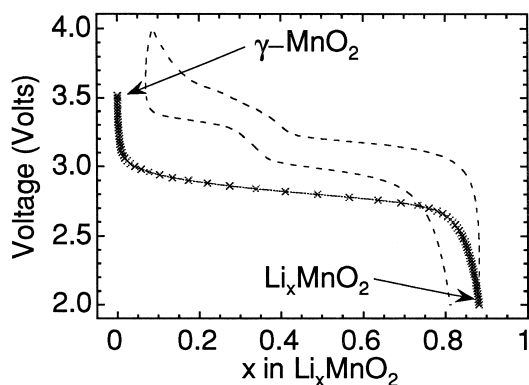


Fig. 4. Curve  $U-x$  of a HTMD sample with Pr = 45% and Mt = 8%, in the 2–4 V range, with a 20 mV/h scanning rate. The first discharge is plotted in full line.

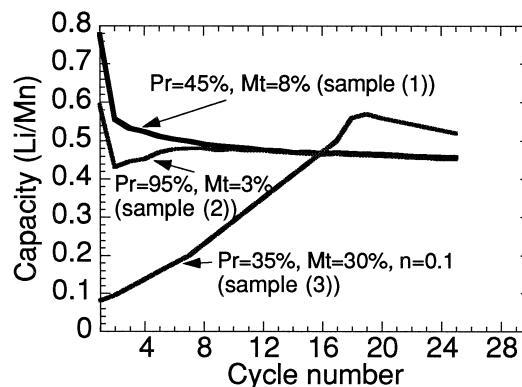


Fig. 5. Influence of de Wolff defects and structural water on the cycling behavior.

Mt = 30%,  $y = 2$ ,  $n = 0.1$ ) which corresponds to an electrodeposited  $\gamma$ -MnO<sub>2</sub> subjected to a mild dehydration process at 100°C under vacuum for several hours, a treatment that ensures the elimination of adsorbed water. It appears that the capacity increases over about 20 cycles before it starts decreasing. The maximum capacity obtained for sample (3) compares well with that of anhydrous samples. It must be mentioned, however, that this capacity is obtained provided the first 20 cycles are done at a slow rate (20 mV/h).

An overview of the simultaneous influence of the structural parameters, Pr and Mt, on the Li insertion behavior appears in Fig. 6, which gives the maximum reversible capacity obtained at a rate of C/100 for lithiated compounds (electrochemically prepared from samples with  $y = 2$ ). It shows that the largest capacities are obtained for

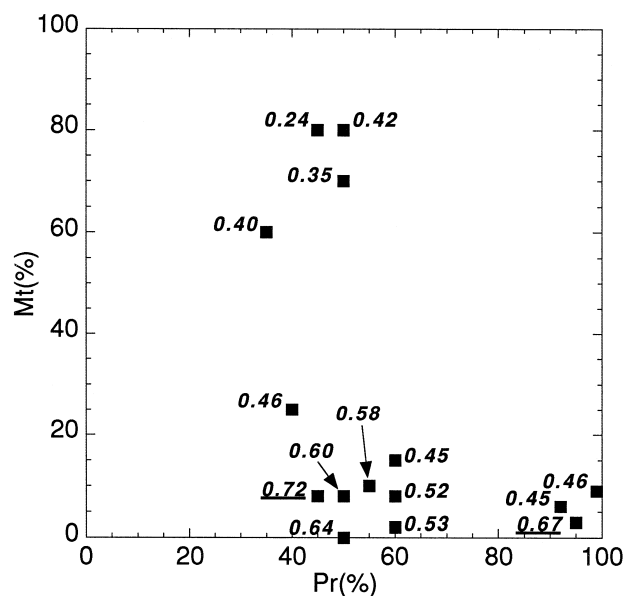


Fig. 6. Maximum Li insertion capacity (in Li/Mn) of lithiated phases obtained from starting  $\gamma$ -MnO<sub>2</sub> with  $y = 2$  and characterized by their structural parameters Pr and Mt.

starting  $\gamma$ -MnO<sub>2</sub> materials with low Pr and Mt values, except for  $\gamma$ -MnO<sub>2</sub> with Pr > 90% and a very small Mt degree.

#### 4. Conclusion

$\gamma$ -MnO<sub>2</sub> materials have been prepared by oxidative electrodeposition under various conditions and subjected to different thermal treatments. It has been shown that their MnO<sub>y</sub>, nH<sub>2</sub>O formulas and structural characteristics (in terms of concentration of De Wolff defects and rate of microtwinning) depends on the synthesis conditions. These can then be adjusted to some extent, so as to obtain a material with desired physico-chemical and structural parameters. For example, a mild thermal treatment enables us to dehydrate a  $\gamma$ -MnO<sub>2</sub> while minimizing its evolution toward a  $\beta$ -MnO<sub>2</sub> structure.

The first Li insertion into  $\gamma$ -MnO<sub>2</sub> materials induces an irreversible transformation leading to lithiated compounds exhibiting a reversible intercalation behavior that strongly depends on the physico-chemical and structural characteristics of the starting materials.  $\gamma$ -MnO<sub>2</sub> with low Pr and Mt values, as well as  $\gamma$ -MnO<sub>2</sub> with Pr > 90% and a very

small Mt value, lead to lithiated phases with the largest reversible intercalation capacities.

#### References

- [1] Y. Chabre, J. Pannetier, Prog. Solid St. Chem. 23 (1995) 1.
- [2] J.M. Cowley, Diffraction Physics, New York, London, DIFFAX VI.76, 1990.
- [3] A. Le Gal La Salle, S. Sarciaux, A. Verbaere, D. Guyomard, Y. Piffard, J. Electrochem. Soc., submitted.
- [4] K.J. Vetter, N. Jaeger, Electrochim. Acta 11 (1966) 401.
- [5] S. Sarciaux, Thesis, Université de Nantes, France, January, 1998.
- [6] A. Verbaere, S. Sarciaux, A. Le Gal La Salle, D. Guyomard, Y. Piffard, to be published.
- [7] T.N. Andersen, Progress in Batteries and Battery Materials 11 (1992) 105.
- [8] R. Williams, R. Fredlein, G. Lawrence, D. Swickels, C. Ward, Progress in Batteries and Battery Materials 13 (1994) 102.
- [9] P. Ruetschi, J. Electrochem. Soc. 131 (1984) 2737.
- [10] C. Poinson, J.-M. Amarilla, Y. Chabre, J. Pannetier, Journées d'Electrochimie, Montréal, Canada, 1997, CO5-7.
- [11] T. Ohzuku, J. Kato, K. Sawai, T. Hirai, J. Electrochem. Soc. 138 (1991) 2556.
- [12] N. Ilchev, V. Manev, A. Nassalevska, J. Power Sources 25 (1989) 167.
- [13] J.B. Fernandes, B.D. Desai, V.N. Kamat Dalal, J. Power Sources 15 (1985) 209.